Jour. Sci. Hiroshima Univ., Ser. C, Vol. 10, No. 3, 487-507 (1995)

Mineralogical Characteristics of Smectite from the Landslide Area in the Neogene Kobe Group, Southwest Japan

by

Taro YASUOKA, Ryuji KITAGAWA
Setsuo TAKENO and Syunji YOKOYAMA

with 5 Tables, 22 Text-figures and 6 Plates

(Received, June 6, 1995)

Abstract: This paper deals with smectite collected from the landslide area in the Neogene Kobe Group, southwest Japan. Samples were collected from throughout the region where the Kobe group was distributed. At the Kinkai area, clear outcrops are developed in which landslides horizon is recognizable. Therefore, numerous samples were collected in the Kinkai area and examined in detail.

Collected samples were first investigated by X-ray powder diffraction method. Among clay minerals, smectite was further inspected by Greene-Kelly test and by chemical analysis. In order to clarify mineralogical characteristics of smectite, differential thermal analysis, pH measurement and observation by scanning and transmission electron microscopy were carried out.

Obtained mineralogical characteristics of smectite from the landslide area were characterized as follows:

1) Only smectite is confirmed in the sedimentary rocks of Miocene sediments distributed around the landslide area of the Kinkai area as clay constituent minerals and amount of smectite is almost constant regardless of the horizon of the sediments.

2) The smectite is identified to be montmorillonite through mineralogical examinations, such as X-ray powder diffraction method, Greene-Kelly test and chemical analysis.

3) Montmorillonite with high Na+ ration is prevailed in the horizon corresponding to the sliding plane.

4) The montmorillonite is characterized by extraordinary expanding nature and the fact is regarded to be the significant cause of the landslide which occurs commonly in the district.

Based on the mineralogical and chemical characteristics of smectite collected from the landslide area, relations between smectite and landslides were discussed.

CONTENTS

I. Introduction

In Japan, various kinds of the natural disasters have become serious problems due to the recent rapid development of human society. Among geological disasters, the landslide is one of the important disasters causing loss of human life, land and property.

In Japan landslides occur frequently, especially in the region of the Tertiary soft sedimentary rocks. Concerning the landslides many studies have been published mainly from the vie point of geotechnics (e.g. Hayashi and Yamada, 1974; Niizeki, 1976; Sokobiki et al, 1986; Aramaki et al., 1987; Hirota et al., 1987). Among these studies significant role of clay minerals was also pointed out (cf. Yajima, 1979; Shuzuki and Shimada, 1987; Tazaki et al., 1991). However, detailed mineralogical examinations on the clay minerals related to the landslides are remained to be solved.

One of remarkably landslide area is situated in the Sanda basin, Hyogo Prefecture. Geology of the basin is composed of the Tertiary Kobe Group. In the basin landslides occur frequently. Huzita and Kasama(1983) studied the landslides of the district and concluded that smectite contained in the sediments play an important role on the landslides.

In this study, clay minerals collected from the landslide area were investigated in detail by X-ray powder diffraction method. These clay minerals were further studied by Greene-Kelly test and chemical analysis. Moreover in order to clarify mineralogical characteristics of smectite, differential thermal analysis, pH measurement and observation by scanning and transmission electron microscopy were carried out.

Based on the mineralogical and chemical characteristics of smectite collected from the landslide area, significant relations between smectite and landslides will be discussed. p73

II. Geological outline

The geological map of the Sanda district is shown in Fig.1 (Kawada et al., 1986). The geology of the district has been investigated in detail by Huzita et al.(1971), Huzita and Kasama(1971), Huzita and Kasama(1983) and Ozaki and Matsuura(1988). According to these papers, the geology of the Kobe group distributed in the district can be summarized as follows:

The Kobe group of the district consists mainly of non-marine sedimentary rocks which unconformably overlies the Arima group. The group is more than 550m thick, and is composed

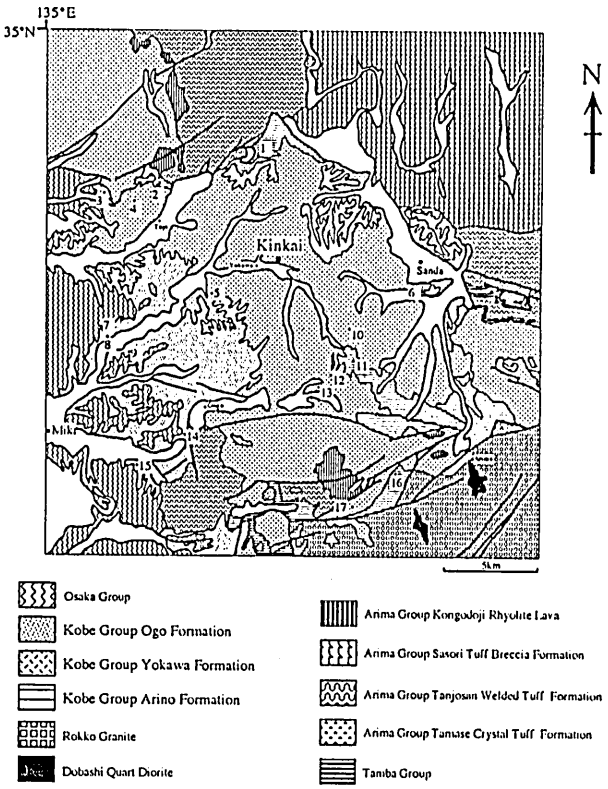

Fig.1. Geological map of the Sanda district together with sampling points (after Kawada et al., 1986; modified partly by the present authors).

of sandstone, mudstone and conglomerate intercalating several thin layers of lignite and rhyolitic tuff. The group is subdivided into the Arino, Yokawa and Oogo formations from the lower to the upper, respectively.

The Kobe group gently dips towards west, showing the kind of imbricate structure throughout the formation. In the investigated area, the upper the formation, distributes more westward, and is covered with the Osaka group unconformably. The Kobe group is believed to be Miocene age on the basis of plant fossils.

III. Samples

Sampling points in this study are also shown in Fig.1. As shown in Fig.1, samples were collected from throughout the region. At the Kinkai area in Fig.1, clear outcrops are developed in which the landslides horizon is recognizable, and more than 60 specimens are collected in this area. The landslides of the area become serious social problem accompanying recent development of the area.

Fig. 2 shows the compiled columnar sections of the Kobe Group (Hujita et al., 1971). The strata distributed in the Kinkai area coincide with the lowest tuff layer of upper Yakawa Formation, which corresponds to the horizon in which landslides occur most fraquently.

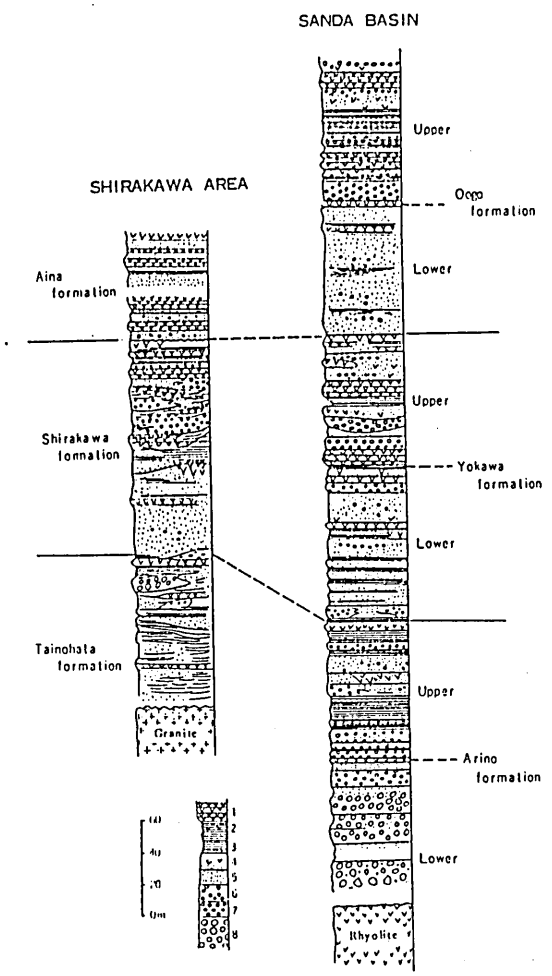

Fig.2. Compiled columnar sections of the Kobe Group (after Huzita et al., 1971).
1: Tuff, 2: TTuffaceous mudstone,
3: Mudstone,
4: Tuffaceous sandstone,
5: Sandstone,
6: Taffaceous conglomerate,
7: Conglomerate (well sorted)
8: Conglomerate (poorly sorted angular gravels)

The distribution of landslides blocks is shown in Fig.3. As is shown in figure, many landslide blocks are developed. The Kinkai area is located in the northeastern part of the map. The distribution of landslide blocks well coincide with the region of the tuff layer of upper Yokawa Formation (Hirota et al.,1987).

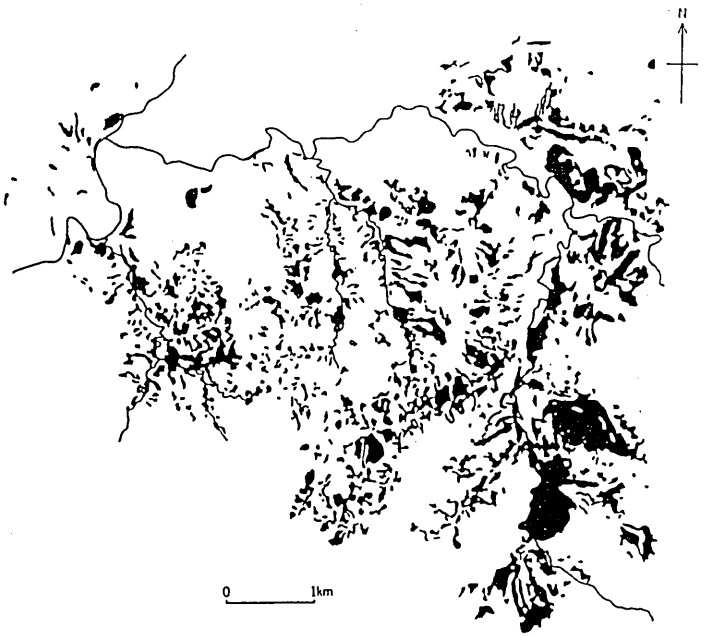

Fig.3. Distribution of landslide blocks in the Sanda basin (after Hirota et al., 1987)

Plates 1 and 2 show the aerial photograph and the outcrop of the Kinkai area, respectively. The Yellowish tuffaceous mudstone corresponds to the horizon of the landslides. As a whole the Kinkai area is constituted with soft tuffaceous rocks, the thin hard sandstone or tuffaceous rocks are sandwiched between the soft tuffaceous beds.

The schematic columnar section of the Kinkai area is shown in Fig.4. Eight beds of the soft rocks were distinguishable in this area. In this area, bed D is known as the horizon of the landslide.

In this paper, nine representative specimens A,B,C,D,E,F-1,F-2,G and H, collected from the eight beds in the Kinkai area were examined in detail with special attention.

IV. Experiments and results

1. X-ray diffraction analysis(XRD)

In order to clarify the constituent minerals of bulk samples, specimens were examined by XRD. The results of the nine selected samples are shown in Fig.5. As is evident in Fig.5, quartz and feldspar are present in addition to the clay minerals. In Fig.5, the basal reflections of about 15A, 13.6A and 22.9A correspond to those of clay minerals. The samples E and F-1 are characterized by existence of clinoptilorite and mordenite, respectively.

For the purpose of further examinations, clay fractions of respective

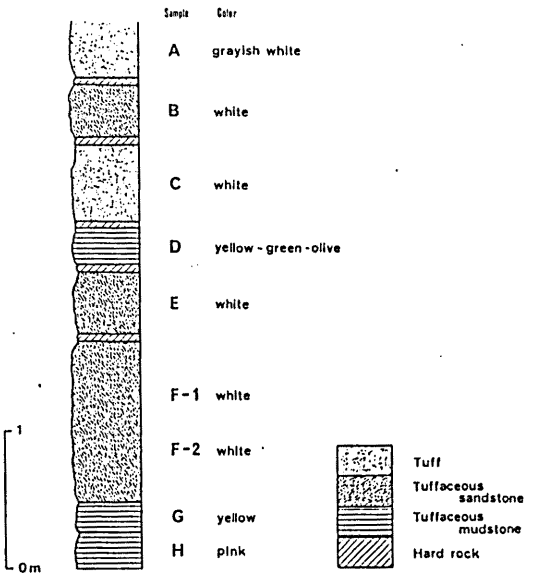

Fig.4. Schematic columnar section of the Kinkai area.

samples were carefully collected by means of water elutriation.

The XRD patterns for the clay fractions are illustrated in Fig.6.

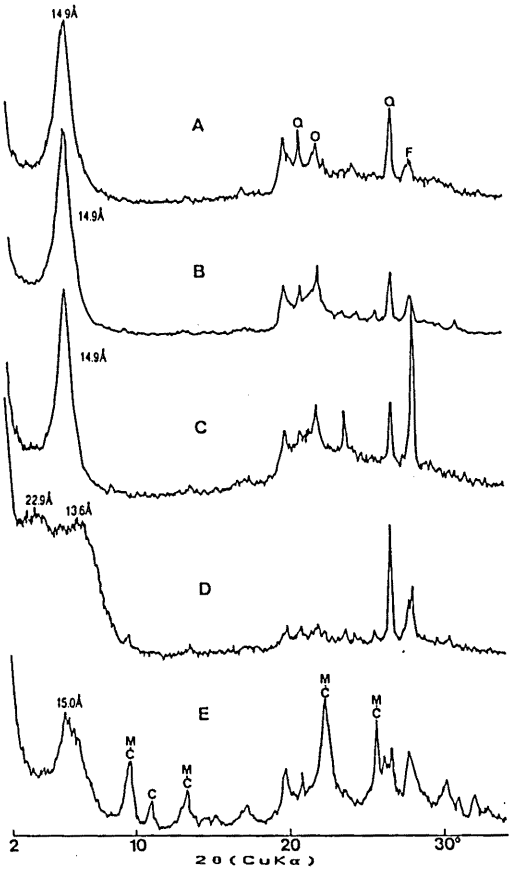

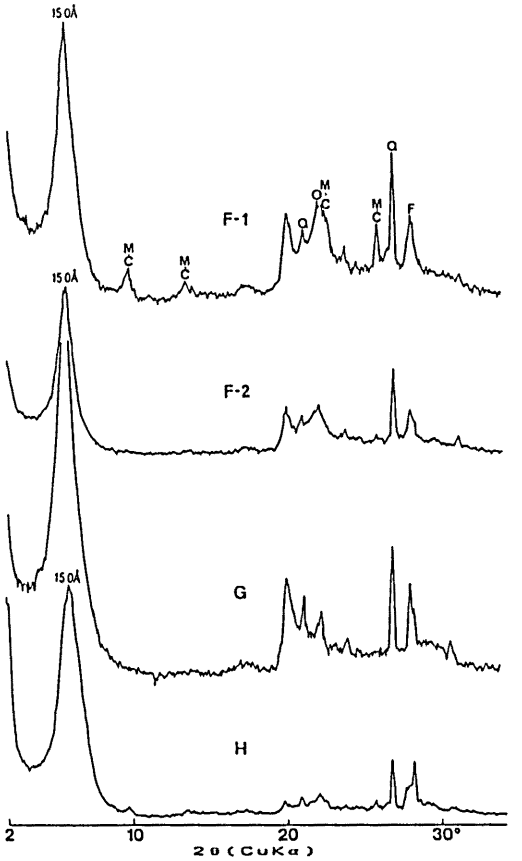

Fig.5. XRD patterns for the respective samples collected from the Kinkai area.
Q: Quartz, O: Opal, F: Feldspar, C: Clinoptilorite, M: Mordenite.

Almost all samples revealed a strong basal reflection at about 15Å. In the samples D and G, broad reflections at about 13Å and 23-24Å are also recognized in addition to the 15A reflection.

For identification of the clay minerals, heating and ethylene glycol and H_2O treatments were carried out on the clay fractions. Heating temperatures were 100°C, 150°C, 200°C and 250°C respectively.

After ethylene glycol treatment, the basal reflections at 15Å of all samples were shifted to about 17Å. After H_2O treatment, the 15Å reflections of most samples were shifted to about 19A with the exception of samples D and G. The basal reflections of samples D and G were shifted to 27.6Å and 23.3Å respectively (Fig.7).

The results of heating treatments are shown in Figs.8 and 9 indicating with increasing the heating temperature, the basal spacing of the respective samples decrease gradually.

As an example of detailed examination of the various treatments, variation of the basal reflection for F-2 are shown in Fig.10. The basal reflection of untreated sample is 15Å. Then with ethylen glycol treatment,

the basal reflection shifted to 16.9Å, with H_2O treatment, it shifted to 18.8Å, after 100oC heating, it shifted to 13.4Å, 150oC heating, 12.3Å, 200oC heating, 11.8Å, 250°C heating, 9.8Å, respectively.

The basal spacing of samples after various treatments are summarized in Table 1. A series of the treatments reveal the characteristics of smectite, and the constituent clay mineral of the nine respective samples was identified as smectite.

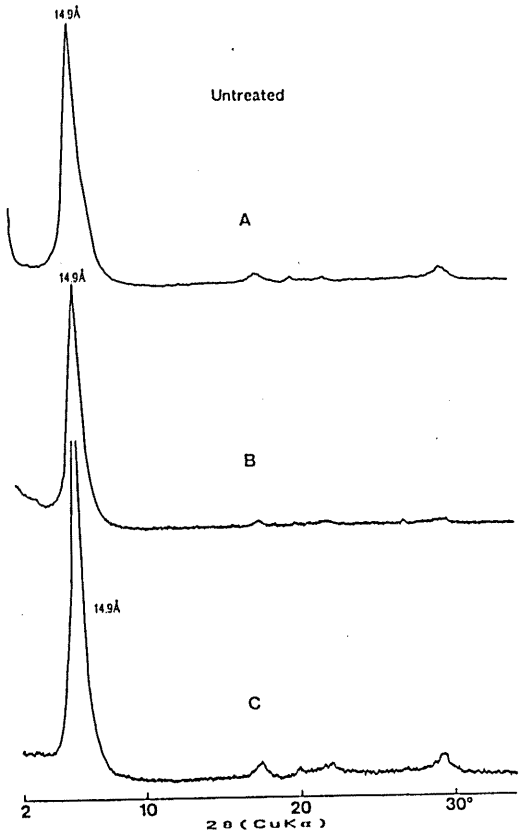

XRD patterns for the clay fractions (<2um).

2. Greene-Kelly test

In order to determine the site of cation substitution, octahedral or tetrahedral sites, Greene-Kelly test (Greene-Kelly, 1955) was applied on the nine representative samples.

Greene-Kelly test is first saturated on Li-saturated smectite and then heating at 300°C for 12 hours and finally treat with glycerol. In smectite, octahedral cations substitution can be confirmed by neutralization of the charge arising from octahedral substitution, through Li

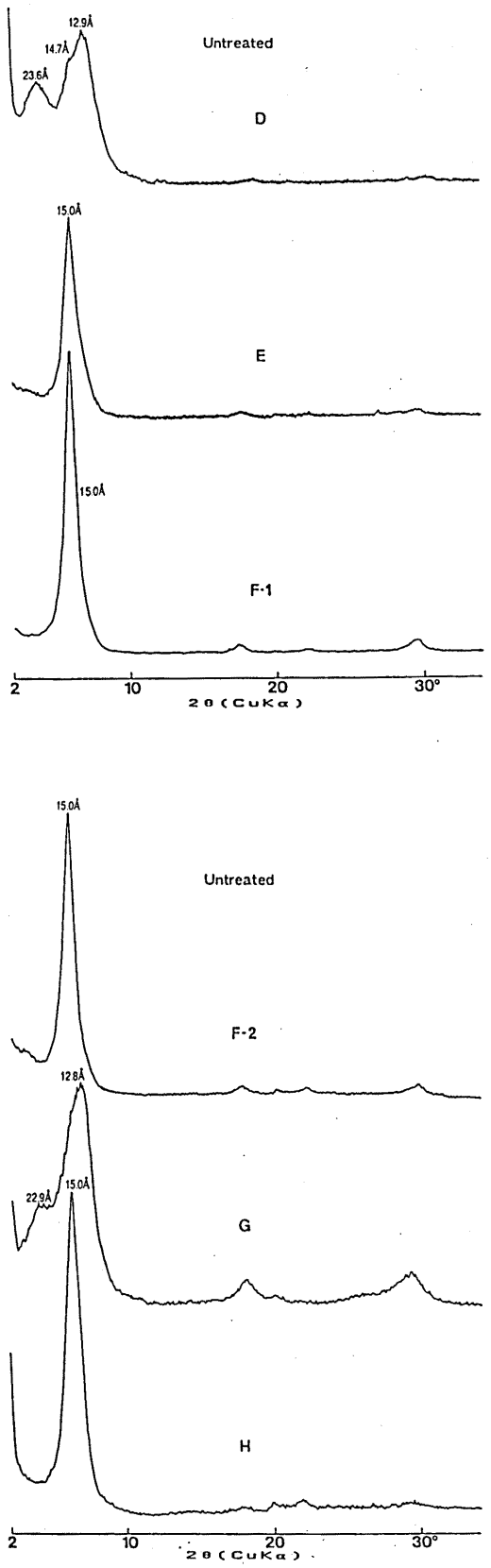

Fig.6. XRD patterns for the clay fractions (<2um).

ions. Tetrahedral cation substitution, on the other hand, can be confirmed by expansibility of the basal spacings. The detailed value can be confirmed by XRD.

The results of the Greene-Kelly test are shown in Fig.11. Almost all specimens indicate a clear reflection at 9.2-9.7Å. However, in sample E, clear reflections are recognized at not only 9.2Å but also 18.8Å. The two reflections suggest both substitutions of octahedral and tetrahedral cations. In samples D and G, clear reflections at 9.6Å and 9.6Å are recognized respectively, in addition to the basal reflections at 17.8Å and 18.8Å respectively. The fact also suggests that the both smectites are formed by mainly octahedrasl cation substitutions accompanying a small amount of tetrahedral substitutions.

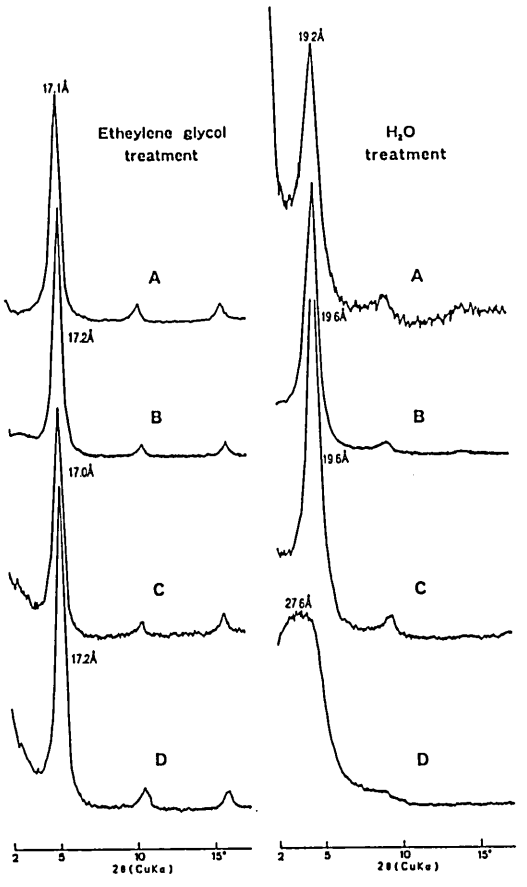

Fig.7. XRD patterns for the clay fractions (<2um) treated with ethylene glycol and H_2O, respectively.

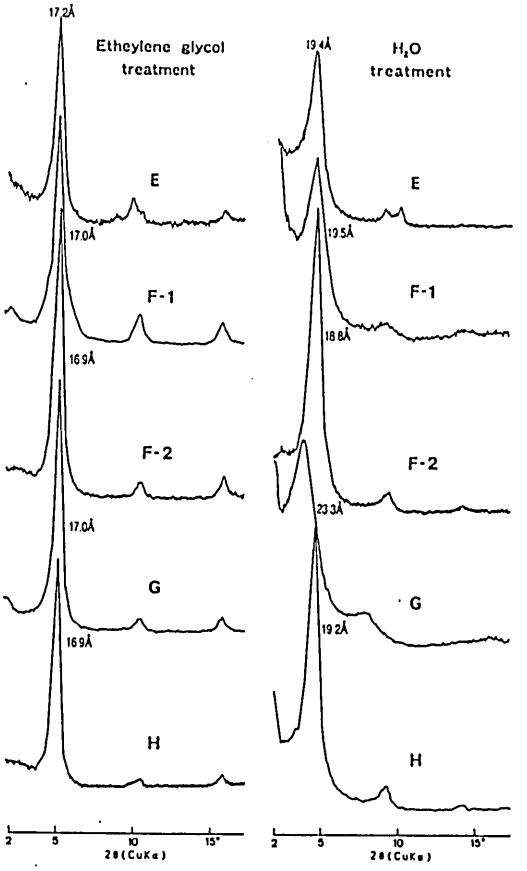

XRD patterns for the clay fractions (<2um) treated with ethylene glycol and H_2O, respectively.

3. Chemical analysis

Chemical characteristics of the smectite were examined by atomic absorption spectrometry. This is because that the mineral species of smectite can be identified by chemical composition (Table 2). The experimental procedure are as follows:

To obtain the solution for atomic absorption measurements three types of method were used, i.e., hydrofluoric-hydrochloric acids solution, hydrofluoric-sulfuric acids solution and alkali fusion methods.

a. Hydrofluoric-hydrochloric acids solution method.

About 100mg of specimens (less than 2um clay fractions) were dissolved in mixed hydroflouric and hydrochloric acids and 50ml or 100ml solutions were obtained with which atomic absorption method was applied. Using the atomic absorption spectrophotometer, contents of Ti, Al Fe, Mn, Mg, Ca, Na, K, Co, Ni, Cu, Zn, Pb, Li, Rb and Sr were measured (Inoue et al., 1987; Imaoka et al., 1987).

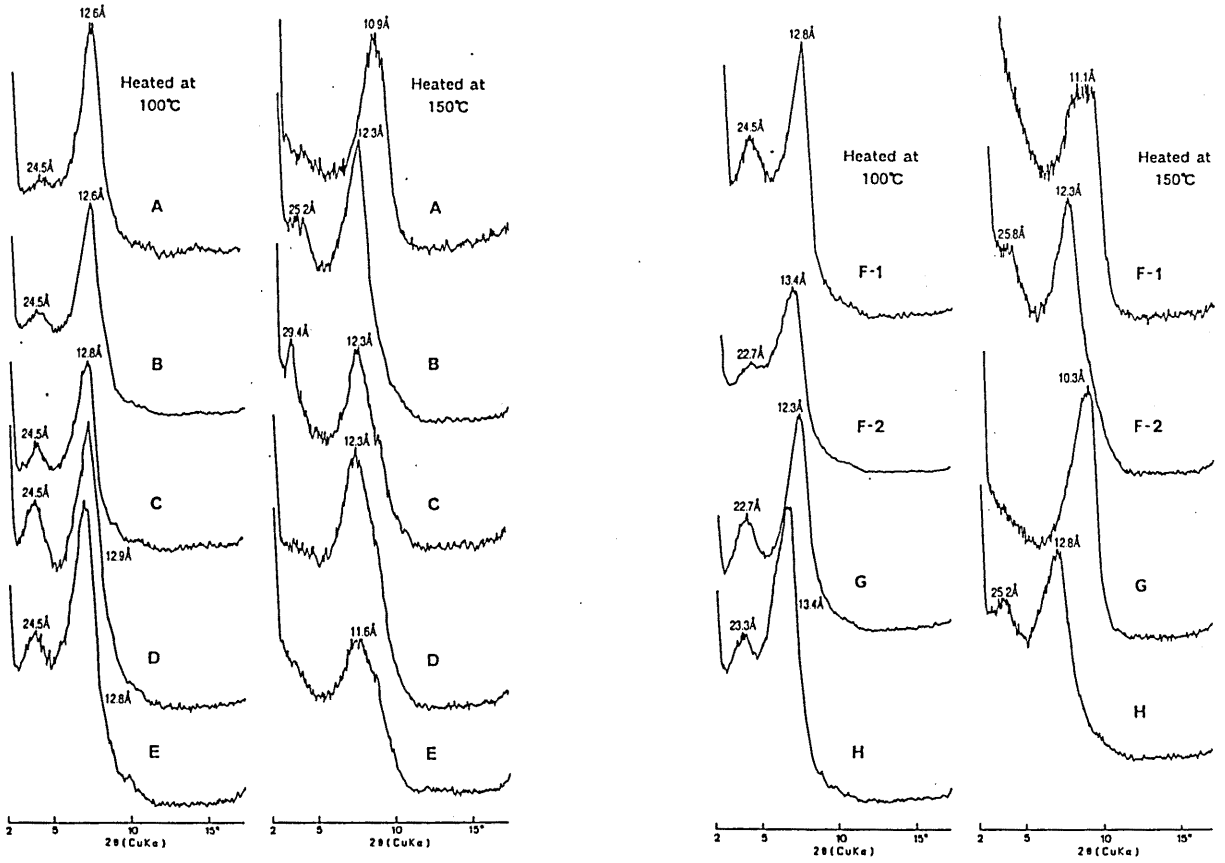

Fig.8. XRD patterns for the clay fractions (<2um) heated at 100°C and 150 C for one hour, respectively.

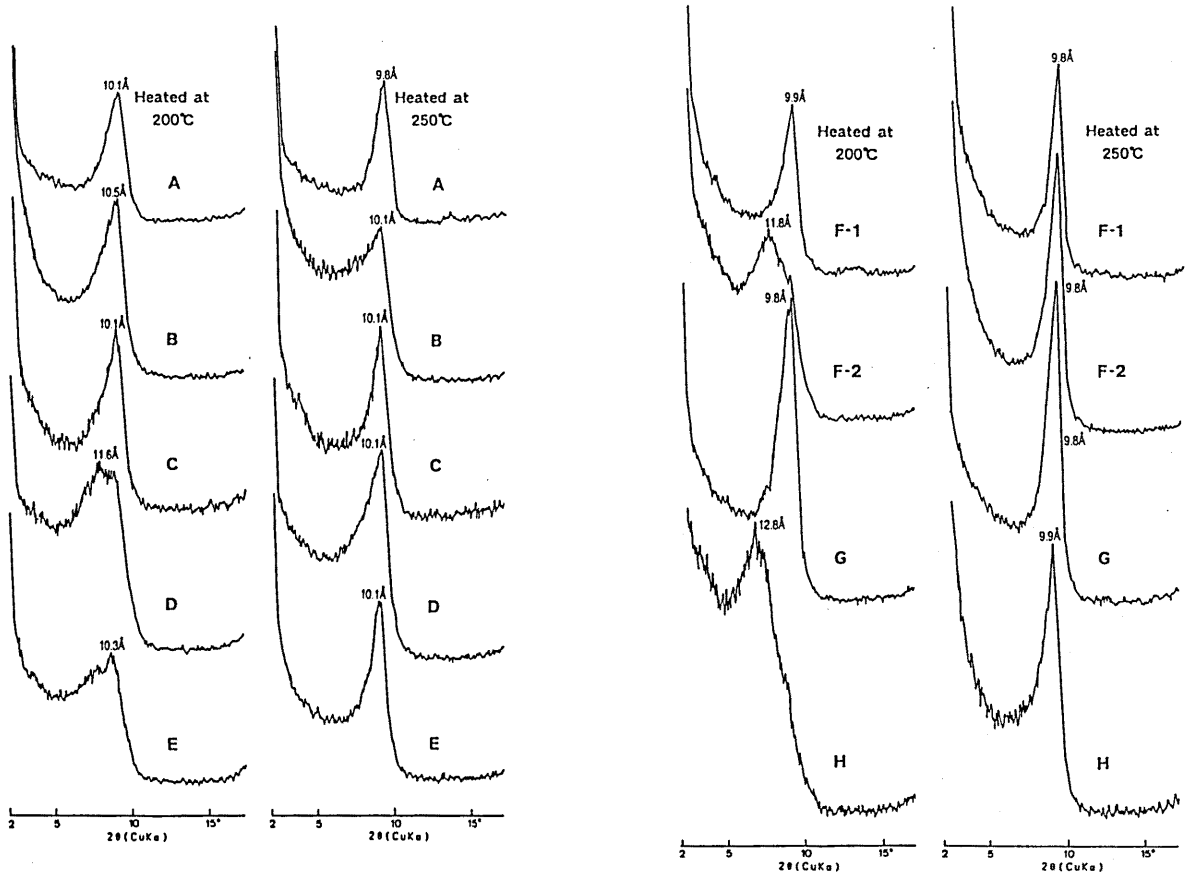

Fig.9. XRD patterns for the clay fractions (<2um) heated at 200°C and 250°C for one hour, respectively.

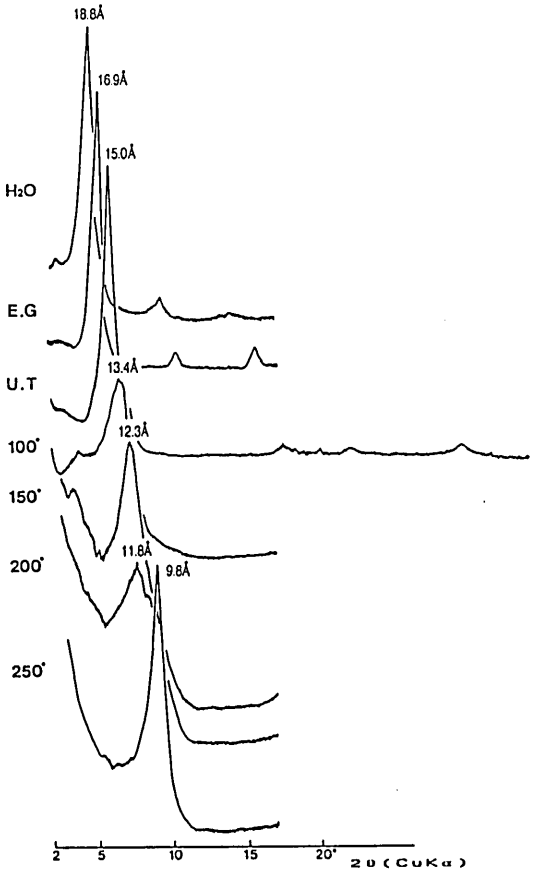

Fig.10. Basal reflections of sample F-2 after various treatment.

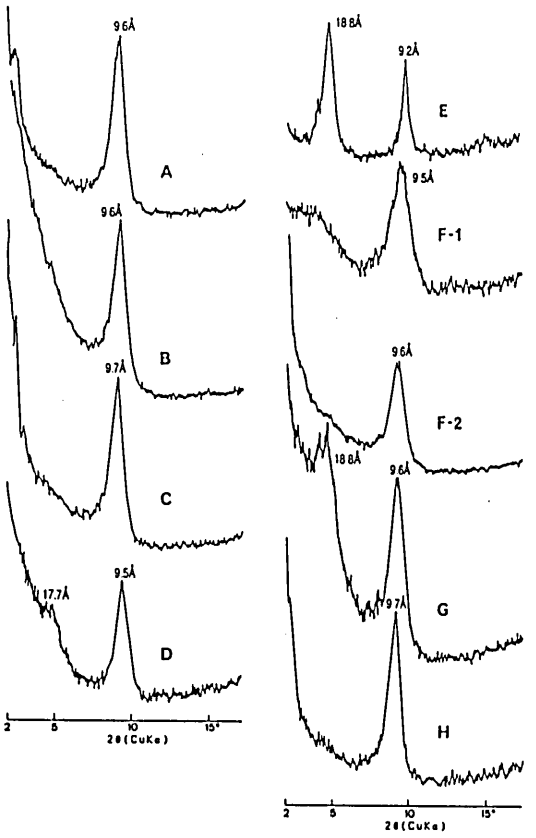

Fig.11. XRD patterns of Li-saturated smectite heated at 300°C and glycerol treatment (Greene-Kelly test).

Sample	Untreated	Heated at 100(°C)	Heated at 150(°C)	Heated at 200(°C)	Heated at 250(°C)	Ethylene glycol treated	R.H.100% treated
A	14.9	12.6(24.5)	10.9	10.1	9.8	17.1	19.2
B	14.9	12.6(24.5)	12.3(25.2)	10.5	10.1	17.2	19.6
C	14.9	12.8(24.5)	12.3(29.4)	10.1	10.1	17.0	19.6
D	12.9,14.7(23.6)	12.9(24.5)	12.3	11.6	10.1	17.2	27.6
E	15.0	12.8(24.5)	11.6	10.3	10.1	17.2	19.4
F-1	15.0	12.8(24.5)	11.1	9.9	9.8	17.0	19.5
F-2	15.0	13.4(22.7)	12.3(25.8)	11.8	9.8	16.9	18.8
G	12.8(22.9)	12.3(22.7)	10.3	9.8	9.8	17.0	23.3
H	15.0	13.4(23.3)	12.8(25.2)	12.8	9.9	16.9	19.2

Table 1. Basal spacing (A) of smectite after various treatment.

Table 2. Classification of smectite (after Güven, 1988).

Ratio between tetrahedral (Xt) and octahedral (Xo) changes	DIOCTAHEDRAL SMECTITES: Predominant octahedral cation(s)	DIOCTAHEDRAL SMECTITES: Smectite species	TRIOCTAHEDRAL SMECTITES: Predominant octahedral cation(s)	TRIOCTAHEDRAL SMECTITES: Smectite species
Xo/Xt>1.0 charges (octahedral predominant)	Al(R^{2+})*	montmorillonite	Mg	stevensite
			Mg(Li)*	hectorite
			AlMgLi	swinefordite
Xt/Xo>1.0 changes (tetrahedral predominant)	Al	beidellite	Mg	saponite
	Fe^{3+}	nontronite	Fe^{2+}	iron saponite
	Cr^{3+}	volkoskoite	Zn	sauconite.
	V^{3+}	vanadium smectite	Mn	manganese smectite

* octahedral substitutions

b. Hydrofluoric-sulfuric acids solution method.

About 100mg of samples was dissolved in mixed hydroflouric and hydrochloric acids and 50ml solution were obtained for examination of Cr content (Imaoka et al., 1987).

c. Alkali fusion method

About 2g sodium carbonate (Na_2CO_3) and 0.3g of boric acid (H_3BO_3) were mixed with about 100mg powdered samples. After fusion in platinum crucible about one hour, 100ml solution was obtained. Using the same machine described above, Si content was measured (Minami, et al., 1978).

Table 3 shows the chemical composition of the clay fractions. Among the major elements, Al, Fe and Mg are believed to be occupied the octahedral site. The Al_2O_3 content is the highest among three elements, in the range from about 13wt% to 19wt%. Fe_2O_3 and MgO contents are in the range from about 1wt% to 5wt%. Taking into account of the data by Greene-Kelly test, the present results indicate that the smectite from the Kinkai area is dioctahedral smectite, that is to say, montmorillonite (Uno, 1992).

Based on 22 minas charge per unit (Takeshi and Uno, 1979; Takeshi and Uno, 1980), the structural formula of the specimen D montomorillonite is obtained as follow:

$$(Ca_{0.10}N_{0.10})(Al_{1.48}Fe_{0.25}Mg_{0.28}Ti_{0.01}Mn_{0.01})(Si_{3.89}Al_{0.11})O_{10}(OH)_{22}\ nH_2O$$

Similarly sample G montmorillonite is expressed as follows:

$$(Ca_{0.13}Na_{0.08}K_{0.02})(Al_{1.51}Fe_{0.2}Mg_{0.26}Ti_{0.02}Mn_{0.01})(Si_{3.90}Al_{0.10})O_{10}(OH)_2\ nH_2O$$

The layer charges of D and G montmorillonites are determined as 0.3 and 0.36 respectively, and the value indicate extensive substitution of octahedral cations of D and G montmorillonite compared with that of tetrahedral cations.

Fig.12 shows variation of major element contents of the samples collected from the Kinkai area. Si is the only tetrahedral cation, whereas Al can occupy both the tetrahedral and octahedral positions. SiO_2 contents of samples D, F-2 and G are relatively low, on the contrary, Al_2O_3 contents of those are relatively high. Fe_2O_3 contents of samples D and G are very high, and MgO content of sample D is relatively high.

Variation of trace element contents of the same samples is illustrated in Fig.13. Extraordinary high content of Sr in sample E is characteristic. However, no other characteristics elements are recognized in the figure.

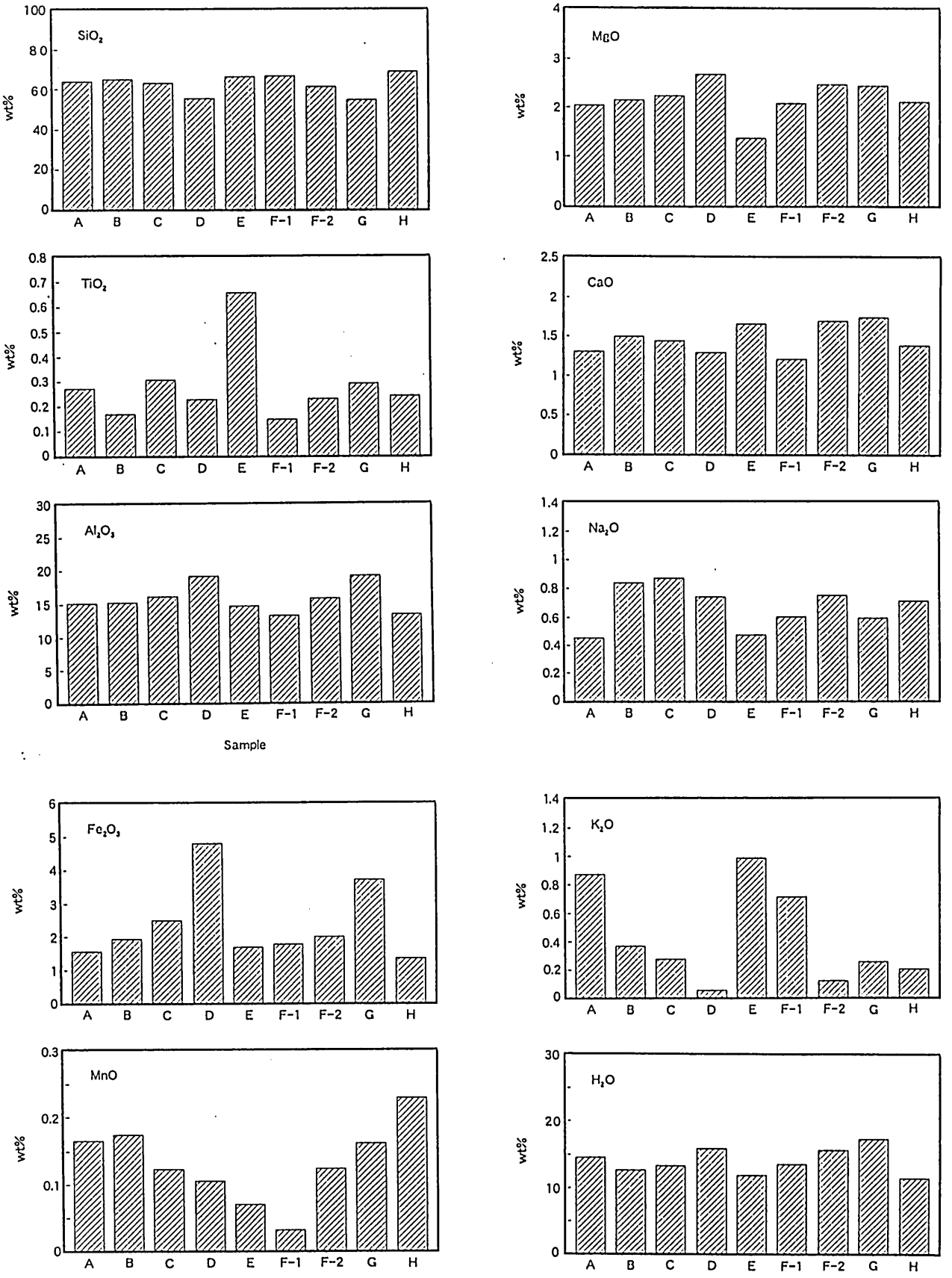

Fig.12. Variation of major element contents of the nine representative samples (<2um).

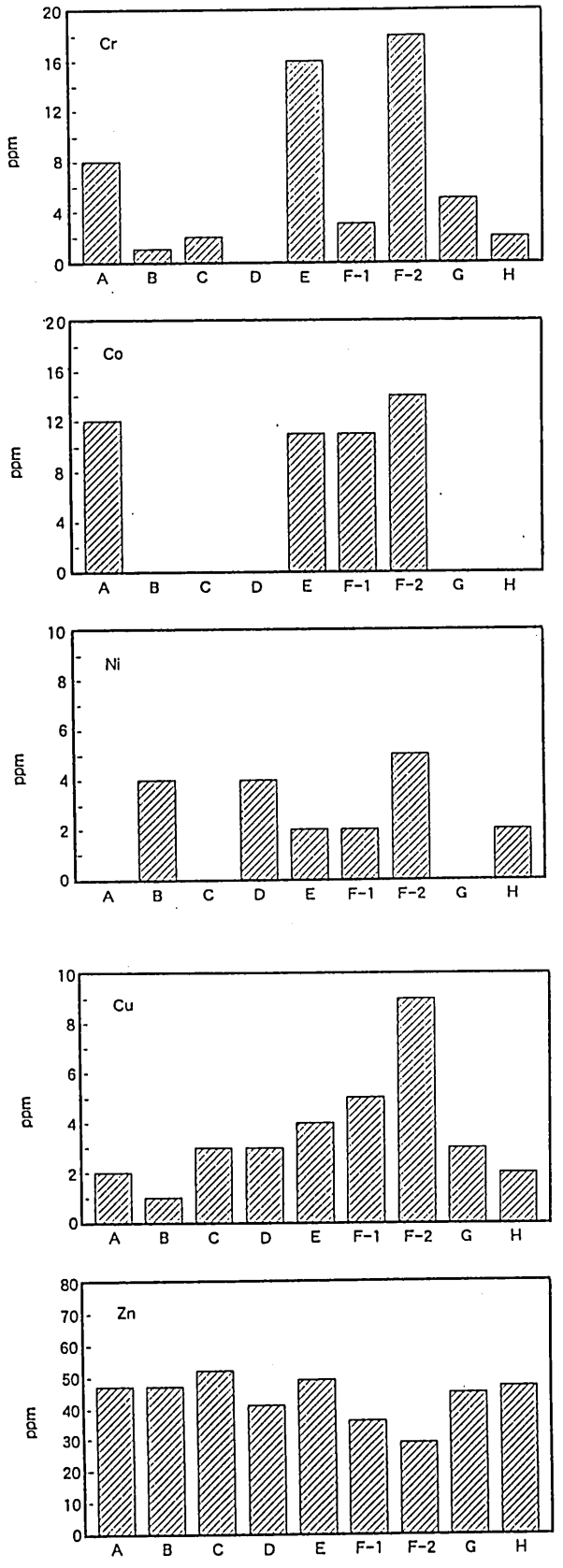

Fig.13. Variation of trace element contents of the nine respective samples (<2um).

4. Differential thermal analysis(DTA)

In order to examine the dehydration temperature of interlayer water and structural (OH) of the montmorillonite (Sakamoto, 1986; Kato, 1989), DTA experiments were carried out on the nine selected samples. thermo gravimetry (TG) diagrams were also measured. These experiments were carried out on about 25mg samples with a heating rate of 10°C/min. up to 1100°C.

The results are summarized in Fig. 14 and Table 4. In Fig. 14, three endothermic peaks caused by dehydration are clearly recognized. The peaks at the lowest temperatures appeared from 60°C to 180°C, are referred to N1 and N2 in this paper

Table 3. Chemical composition of the clay fractions (≤2μm) for each sample.

Sample	A	B	C	D	E	F-1	F-2	G	H
(wt%)									
SiO_2	63.76	65.03	62.95	55.17	66.56	66.78	61.24	54.45	69.08
TiO_2	0.27	0.17	0.31	0.23	0.66	0.15	0.23	0.29	0.24
Al_2O_3	15.00	15.21	16.04	19.11	14.63	13.15	15.71	19.10	13.30
Fe_2O_3	1.56	1.93	2.48	4.81	1.68	1.76	2.00	3.72	1.36
MnO	0.17	0.17	0.12	0.11	0.07	0.03	0.12	0.16	0.23
MgO	2.04	2.14	2.24	2.67	1.38	2.08	2.47	2.44	2.11
CaO	1.30	1.49	1.44	1.29	1.66	1.21	1.70	1.75	1.39
Na_2O	0.45	0.83	0.87	0.74	0.47	0.60	0.75	0.59	0.71
K_2O	0.87	0.37	0.27	0.05	0.99	0.72	0.12	0.25	0.20
H_2O	14.58	12.65	13.30	16.05	11.91	13.52	15.67	18.61	11.18
(ppm)									
Cr	8	1	2	0	16	3	18	5	2
Co	12	0	0	0	11	11	14	0	0
Ni	0	4	0	4	2	2	5	0	2
Cu	2	1	3	3	4	5	9	3	0
Zn	47	47	52	41	49	36	29	45	42
Pb	0	0	16	24	42	0	31	54	49
Li	25	29	38	33	21	10	35	41	38
Rb	63	44	47	28	76	48	27	39	50
Sr	89	76	65	87	387	35	85	89	94

and the peaks are caused by interlayer water dehydration. At about 600°C to 700°C, a small peaks is recognized, referred to N3 peak caused by structural (OH) dehydration.

In Table 4 temperatures of N1, N2 and N3 peaks are summarized. Although small variation of temperatures of the peaks are recognizable, temperatures of N1, N2 and N3 peaks of the nine samples are almost constant. That is, montmorillonite of the Kinkai area shows almost similar thermal behavior with each other.

5. Abrasion pH

Abrasion pH values of bulk samples were measured using Degital pH-meter with glass electrode, HM 20B manufactured by Toa Denpa Kogyo Co.LTD. Because of experimental difficulties of measuring abrasion pH of clay minerals in a strict sense, a term "abrasion pH" is defined in this paper. The "abrasion pH" was measured in the following way:

100cc water and 500mg bulk sample were put together into a glass bottle and stirred in the bottle using electric magnet. After twenty minutes, the glass electrode of pH-meter is inserted in the glass bottle for fifteen minutes, and the "abrasion pH" was measured.

Fig. 15 and Table 5 show the results of the abrasion pH experiments. Samples D, F-2 and G indicate alkalinity, with values of more than 8.00, whereas other samples are almost neutrality or weak acidity. As the results, abrasion pH indicate neutrality or alkalinity, abrasion pH indicate neutrality or alkalinity as was reported in the previous literature (Shirozu, 1988).

6. Electron microscopic observation.

Micromorphological characteristics of the montmorillonite were examined by scanning electron microscopy. Transmission electron microscopy was also used to examine more detailed finer morphology of the montmorillonite. Plate 3 and plate 4 show the SEM photographs and TEM photographs of respective montmorillonite. Aggregations of flaky montmorillonite are generally observable in all samples by SEM. The size and morphology of montmorillonite are variable showing irregular and play morphologies. Under the TEM observations, very thin and partly rolled fractions were also recognized.

These results indicate that no remarkable difference is exist among the montmorillonite collected in the Kinkai area.

V. Discussion

1. Constituent clay minerals

Regional variation of the constituent minerals of the examined samples are shown in Fig.16. Relative

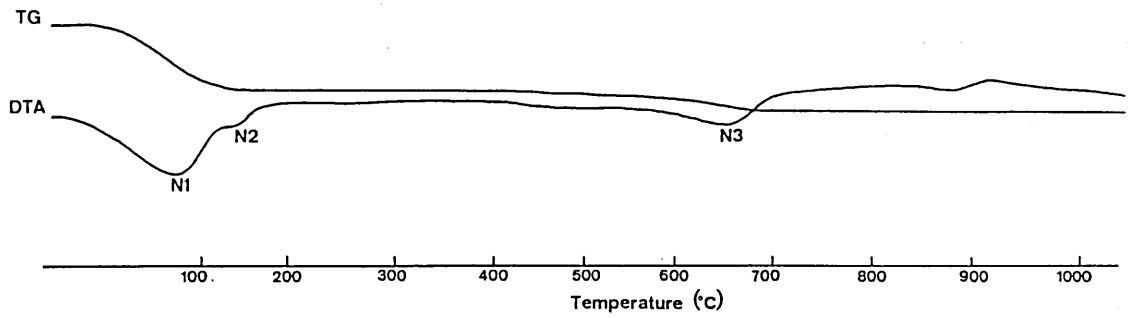

Fig.14. DTA-TG curve for smectite (sample G).

Sample	N1 peak(°C)	N2 peak(°C)	N3 peak(°C)
A	87	141	653
B	86	165	665
C	84	164	690
D	91	166	658
E	67	152	648
F-1	84	150	659
F-2	89	162	669
G	95	143	653
H	82	162	664

Table 4. Temperature of N1, N2 and N3 peaks of the respective samples (DTA).

Sample	pH
A	6.79
B	7.09
C	6.74
D	8.20
E	6.90
F-1	7.02
F-2	9.10
G	8.27
H	6.49

Table 5. Abrasion pH of the samples.

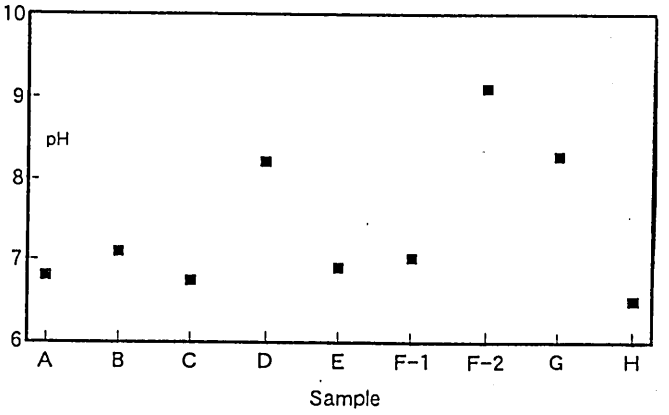

Fig.15. Abrasion pH of the samples.

abundance of minerals were determined by the X-ray powder diffraction method. As is evident in Fig.16, predominance of smectite in all areas should be pointed out. Moreover, samples of points 6, 8 and 17 are composed of almost 100% smectite. Other samples contain small amount of mica clay mineral, kaolin mineral and zeolite in addition to smectite.

To be noted is that only smectite is confirmed in the soft sedimentary rocks corresponding to the landslide horizon in the Kinkai area. In the Kobe Group, predominance of smectite in the landslide area was already pointed out by Huzita and Kasama (1983).

2. Dehydration temperatures

The samples A and G dehydrate at relatively lower temperature (average is about 140°C) than those of other samples. This temperature is referred to N2 in the present paper. The basal reflections of the samples A and G shift to about 10Å with heating treatment at 150°C (Tables 1 and 4).

On the other hand, the dehydration temperatures of the samples D, F-2 and G are rather higher (more than 160°C) than those of the other samples. This temperatures corresponds to N2 peak on the DTA curve. The basal reflections of the samples A and G shift to about 10Å after heating treatment at 250°C which can be confirmed by the X-ray powder diffraction method.

Therefore, the temperature of the N2 peak is correlated closely with the temperature at which the basal reflection shifts to about 10Å. The shift

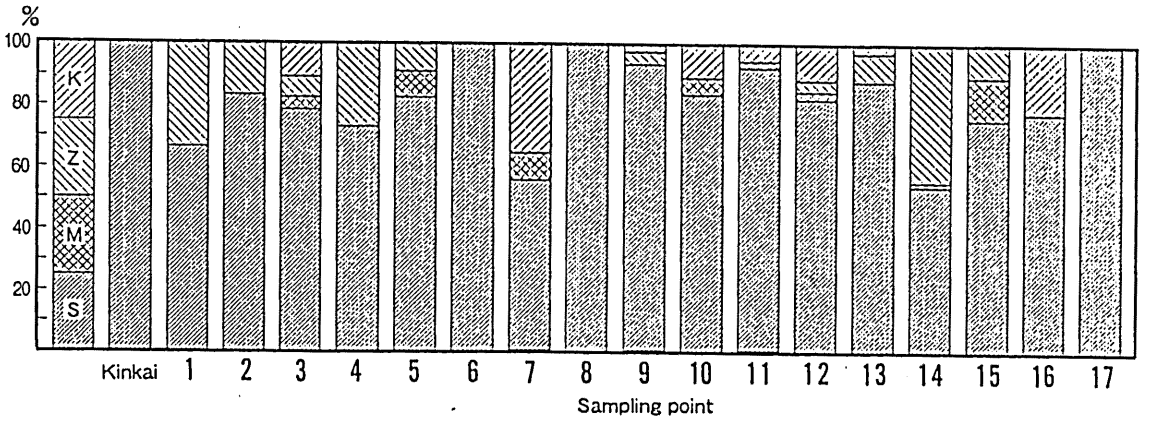

Fig.16. Regional variations of the constituent minerals (<2um) of the examined samples (soft sedimentary rocks).

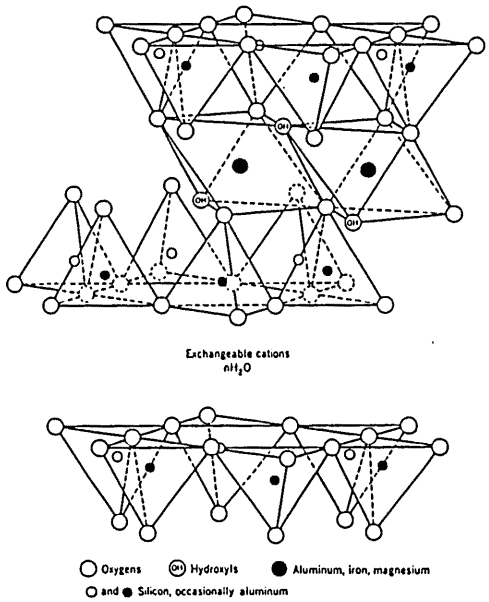

Fig.17. Diagramatic sketch of the structure of smectite (after Grim, 1968).

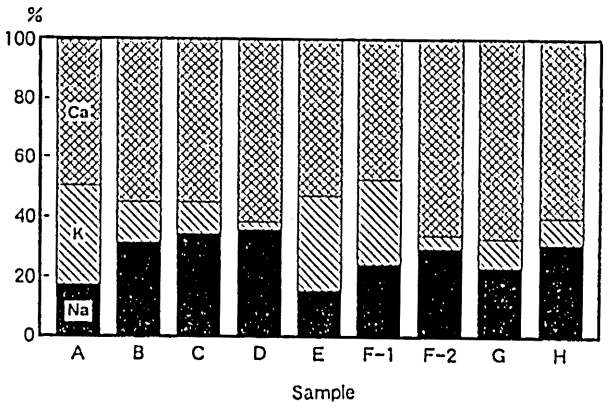

Fig.18. Relative abundance of the interlayer cations in montmorillonite collected from the Kinkai area.

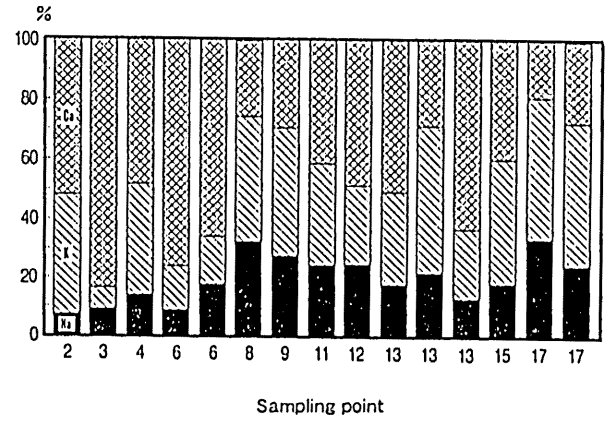

Fig.19. Relative abundance of the interlayer cations in smectite collected from the Kobe Group.

of basal reflection by heating treatment may be certainly caused by the dehydration of the interlayer water. The detailed value of the contraction of the basal spacing is obtained by XRD.

3. Interlayer cations.

Fig.17 illustrates of the structure of smectite (Grim, 1968). The interlayer position of montmorillonite is assigned to exchangeable cations such as Ca2+, K+ and Na+ in addition to H_2O molecules. Si and Al are in general considered to occupy the tetrahedral site. Most of the other elements can occupy the octahedral position.

Fig.18 shows relative abundance

of the interlayer cations of Ca^{2+}, K^+ and Na^+ in montmorillonite collected from the Kinkai area. As is seen in this Figure, the ratios of K^+ of the samples A, E and F-1 against (Ca^{2+} + K^+ + Na^+) are higher than those of the other samples. The basal reflections of these samples shift to about 10Å at lower temperature than that of the other samples. The Ca^{2+} ratios of the samples D, F-2 and H against (Ca^{2+} + K^+ + Na^+) are higher than those of the other samples. The basal reflections of these samples shift to about 10Å at relatively higher temperature than that of the other samples. As is obvious in this Figure, the sample D reveals the highest ratio of Na^+ against (Ca^{2+} + K^+ + Na^+), and the smallest ratio of K^+ against (Ca^{2+} + K^+ + Na^+) among the investigated samples. Moreover, only the basal reflection of this sample shifted to 27.6Å after H_2O treatment.

In summary, montmorillonite of the sample D is characterized as follows:

a. The highest ratio of Na^+ against (Ca^{2+} + K^+ + Na^+).

b. Dehydration temperature is rather high.

c. Higher expansibility than that of the other samples.

Fig.19 shows relative abundance of the interlayer cations (Ca^{2+} + K^+ + Na^+) in montmorillonite collected from the Kobe Group. As is seen in this Figure, the ratio of K^+ against (Ca^{2+} + K^+ + Na^+) in the smectite collected from the other areas tends to be higher than that of montmorillonite collected from the Kinkai area.

4. Interlayer water

Montmorillonite is characterized by interlayer water. The quantity of the interlayer water varies in the range from zero to three molecules according to the difference of the layer charge (Jonas and Roberson, 1966), and also varies according to the varieties of the interlayer cations and the relative humidity in the atmosphere. One molecule of H_2O corresponds to the C axis spacing of about 3Å (Iwasaki, 1979). Watanabe and Sato (1988) studied in detail variations of basal spacing in montmorillonite at various relative humidity, as is shown in Fig.20. They presented the variation of the basal spacings of montmorillonite with different cations (Ca^{2+}, K^+ and Na^+). Their curves are stepwise varied with increasing relative humidity.

Fig.21 shows relationship between the interlayer spacing, d, of montmorillonite in the aqueous emulsions and the water contents, C (Fukushima, 1984). In the region of C>1.0, i.e., more than 100% relative humidity, the d-spacing of Na-montmorillonite increases steadily with increasing water content. Thus, Na-montmorillonite swells infinitely as increasing water content. However, Ca-montmorillonite keeps almost constant d-values with increasing water content. When the sample D is considered, the highest Na ratio against (Ca^{2+} + K^+ + Na^+) reveals the highest among the examined samples (Fig.22). The basal reflection of the sample D shifts to 27.6A by H_2O treatment, with more than 100% relative humidity, and the value corresponds to the state of C=1.1-1.2 in Fig.21.

Fig.22 shows the variation of montmorillonite structure according to the environment (relative humidity). The state of interlayer balance changes with the relative humidity of the environment i.e., water content around montmorillonite, the hydration energy and the electrostatic energy. When the interlayer cation is Na and water content is high (C>; Fig.21), water molecules are introduced into the interlayer position resulting expansion of the interlayer. As a result, the electrostatic energy between Na^+ and silicate-layer becomes small and hydration energy becomes high. In this case water molecules are successively introduced into the interlayer position. Therefore Na-montmorillonite swells infinitely (Iwasaki, 1992).

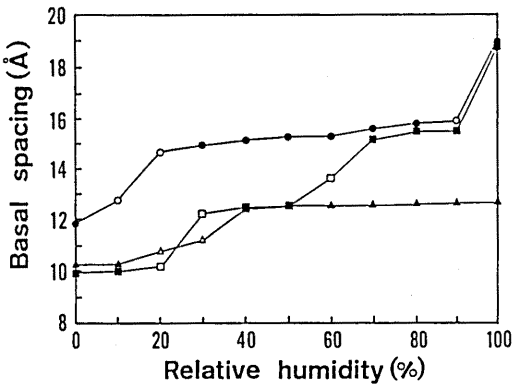

Fig.20. Variations of basal spacing in Na-saturated (■, □), K-saturated (▲, △) and Ca-saturated (●, ○) montmorillonite at various relative humidity. Black symbols: rational basal reflections. Open symbols: irrational basal reflections (after Watanabe and Sato, 1988).

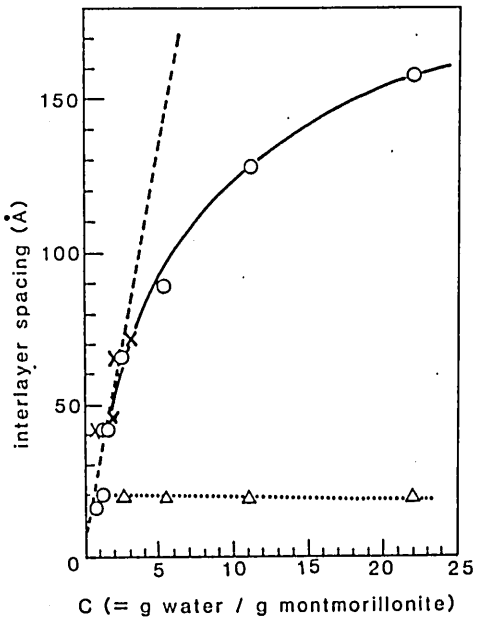

Fig.21. Relationship between the interlayer spacing, d, in the emulsions and the water contents, C: Experimental results of this work; O (Na-montmorillonite and water), Δ (Na-montmorillonite, water and $CaCl_2$ or HCl), Experimental results by Norrish; X , and the calculated result by straight column model;---, and by zig-zag column model; —— , (after Fukushima, 1984).

When the interlayer cation is Ca^{2+} and water content is high (C>; Fig.21), the electrostatic energy between Ca^{2+} and silicate-layer is higher than the hydration energy. In the case of Ca-montmorillonite, maximum water contained in the interlayer position is three molecules (Watanabe and Sato, 1988).

5. Landslide

In the present investigation, the slickenside caused by landslide was confirmed in the D bed. Plate 5 shows the slickenside in the D bed. Hirota et al.(1987) pointed out that the D bed was the sliding plane. The strike and dip of the slickenside measured by the present survey were N30°E and 28°N, respectively. Striations were also observed on the slickenside and the direction of striations was N48°W, 22°N.

If the ground water and the surface water are supplied sufficiently in the Kinkai area, montmorillonite in the D bed will surely be expanding since montmorillonite in the D bed keeps the highest ratio of $Na/(Ca^{+} + K^{+} + Na^{+})$. Therefore, the sliding occurs most probably in the D bed containing such montmorillonite.

Plate 6 shows the D bed after rainfall. The state of dissolution is observed on the surface of the bed. This means montmorillonite in the D bed begins to swell.

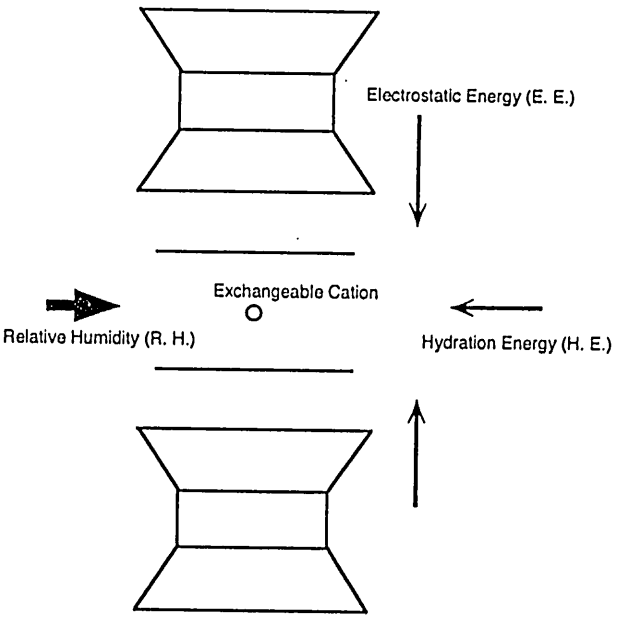

Fig.22. Variation of montmorillonite structure according to the environment (relative humidity).

V. Conclusion

Mineralogical characteristics of smectite from the landslide area in the Neogene Kobe Group, southwest Japan are summarized as follows:

Only smectite is confirmed in the sedimentary rocks of Miocene sediments distributed around the landslide area of the Kinkai area as clay constituent minerals and amount of the content of smectite is almost constant regardless of the horizon of the sediments.

The smectite is identified to be montmorillonite by detailed clay mineralogical examinations such as X-ray powder diffraction method, Greene-Kelly test and chemical analysis.

The interlayer cations of the montmorillonite are confirmed to be Ca^{2+}, Na^{+} and K^{+}. Moreover, remarkably high Na ratio is recognized in the horizon corresponding to the landslide.

The montmorillonite is characterized by extraordinary expanding nature and the fact is considered to be the important cause of landslide which occurs commonly in the district.

References

Aramaki, S., Kitazono, Y., Suzuki, A. and Kajiwara, M.(1987): On physical properties of soils weathered from Tertiary sedimentary rock on Amakusa island. Jour. Japan Soci. Eng. Geol., 28, 193-200*

Fukushima, Y. (1984): X-ray diffraction study of aqueous montmorillonite emulsions. Clays Clay Miner., 32, 320-326.

Greene-Kelly, R. (1955): Dehydration of the montmorillonite minerals. Miner. Mag., 30, 604-615.

Grim, R.E. (1968): Clay mineralogy, 2nd ed., Mcgraw-Hill book Co., New York, pp79.

Guven, N.(1988): Smectite: in hydrous phyllosilicates, S.W. Bailey ed., Reviews in Mineralogy, 19, Miner. Soci. Amer., Washington, D.C., pp497-559.

Hayashi, Y. and Yamada, T. (1974): On the mineral compositions and the physical properties of mud-stones of Kobe Group (Miocene). Eng. Geol., 15, 99-104.*

Hirata, K., Sasaki, I. and Tanioka, T.(1987): Relationship between landslide and geology with geographical feature in the Neogene Kobe Group (Yokawa-cho in southern Hyogo, Japan). Geol. Rept. Shimane Univ., 6, 119-130.*

Huzita, K., Kasama, T. (1971): Geologic map around the Rokko mountains (1/50000) and its explanation. Kobe city.**

Hizita, K. and Kasama, T. (1983): Geology of the Kobe district. Quad rangle series, scale 1:50,000, Geol. Surv. Japan, pp115.*

Huzita, K., Kasama, T., Hirano, M., Shinoda, T. and Yamashita, M. (1971): Geology and geomorphology of the Rokko area, Kinkai district, Japan -with special reference to Quaternary tectonics-. Jour. Geosci. Osaka city Univ., 14, 71-124.

Imaoka, T., Inoue, K. and Minami, A.(1985): Determination of trace elements in the silicate rocks by atomic absorption spectrophotometry-used Shimazu AA-646-. Prof. H. Yoshida Memorial, 322-332.**

Inoue, K., Ikeda, Y. and Minami, A.(1985): Determination of sodium, potassium, magnesium and iron in the silicate rocks by atomic absorption spectrophotometry- used Shimazu AA-646-, Prof. H. Yoshida Memorial, 355-363.**

Iwasaki, T. (1979): Relationship between X-ray basal reflections and interlayer cations of montmorillonite: on the distribution of Ca and Na ions, Jour. Miner. Soci. Japan, 14, Special issue, 78-89. *

Iwasaki, T (1992): Smectite and zeolite: In Resouce geology; The year 2000, S. Ishihara, T. Urabe and N. Shikazono, eds., Resource Geol. Tokyo, Japan, 143-150.*

Jonas, E.C. and Roberson, H.E.(1966): Stractural change density as indicated by montmorillonite hydration. Clays Clay Miner., 13, 223-230.

Kato, C.(1989): Condition of adsorbed water, interlayer water and constitution water of clay minerals, Jour. Clay Sci. Soci. Japan, 29, 118-128.*

Kawada, K., Miyamura, M. and Yoshida, F.(1986): Geological map of the Kyoto-Osaka district, Scale 1:200,000, Geol. Surv. Japan.

Minami, A., Inoue, K. and Fujii, I.(1987): Determination of major elements (Si, Al) in the silicate rocks by atomic absorption spectrophotometry -with special reference to the analysis of rocks rich in aluminum silicates (pyrophyllite)-. Prof. Satoru Kakitani Memorial, 106-112.**

Niizeki, A.(1976): On the landslide in Kinki. Eng. Geol. 17, 62-75.*

Ozaki, M. and Matsuura, H.(1988): Geology of the Sanda district. Quad rangle series, scale 1:50,000, Geol. Surv. Japan, pp93.*

Sakamoto, T.(1986): Differential thermal analysis of smectite-with special reference to endothermic peaks around 100oC-. Special issue, 147-153.*

Shirozu, H. (1988): Introduction to clay mineralogy-fundamentals for clay science-, Asakura-shoten Co., Tokyo, pp185.**

Shuzui, H. (1984): The rock block slide at Hitotsu-Tsubota, Fukushima Prefecture-Especially on the characteristics of clay minerals and quality of groundwater-, Jour. Japan Soci. Eng. Geol., 25, 23-33.*

Shuzui, H. and Shimoda, s.(1987) Clay minerals of landslide clays in the Kunimi area, Toyama Pref., Jour. Clay Sci. Soci. Japan, 27, 211-220*

Sokobiki, H., Kobashi, S. and Habara, T.(1986): Studies on dabris-flow in Rokko district (part 2), Jour. Japan Soci. Eng. Geol., 27, 119-127.*

Takeshi, H. and Uno, Y.(1979): Notes on the formation and transformation of montmorillonites in Japan, Jour. Miner. Soci. Japan, 14, Special Issue, 70-77.*

Takeshi, H. and Uno, Y.(1980): Mineralogical properties and transformation of montmorillonites, Jour. Clay Sci. Soci. Japan, 20, 67-78.*

Tazaki, K., Kitayama, S., Nagami, A. and Yang, P.C.(1991): Clay mineralogy on landslides in Teragi area, northern Hyogo, Japan, Geol. Rept. Shimane Univ., 10, 39-45.*

Uno, Y.(1992): Smectite in bentonite deposits, Black Hills Wyoming, Jour. Clay Sci. Soci. Japan, 31, 202-211.*

Watanabe, T. and Sato, T.(1988): Expansion characteristics of montmorillonite and saponite under various relative humidity conditions, Clay

Sci., 7, 129-138.
Yajima, S. (1979): The relation between clay minerals at landslide area and landsliding, Jour. Clay Sci. Soci. Japan, 19 91-96.*

*:in Japanese with English abstract
**:in Japanese

Taro YASUOKA, Ryuji KITAGAWA and Setsuo TAKENO:
Department of Earth and Planetary Systems Science, Faculty of Science, Hiroshima University, Kagamiyama, Higashihiroshima 739, Japan.

Syunji YOKOYAMA:
Technical Research Institute, Kawasaki Geological Engineering, Co.,LTD, 1-11-8, Motomachi, Naniwa-ku, Osaka 556, Japan.

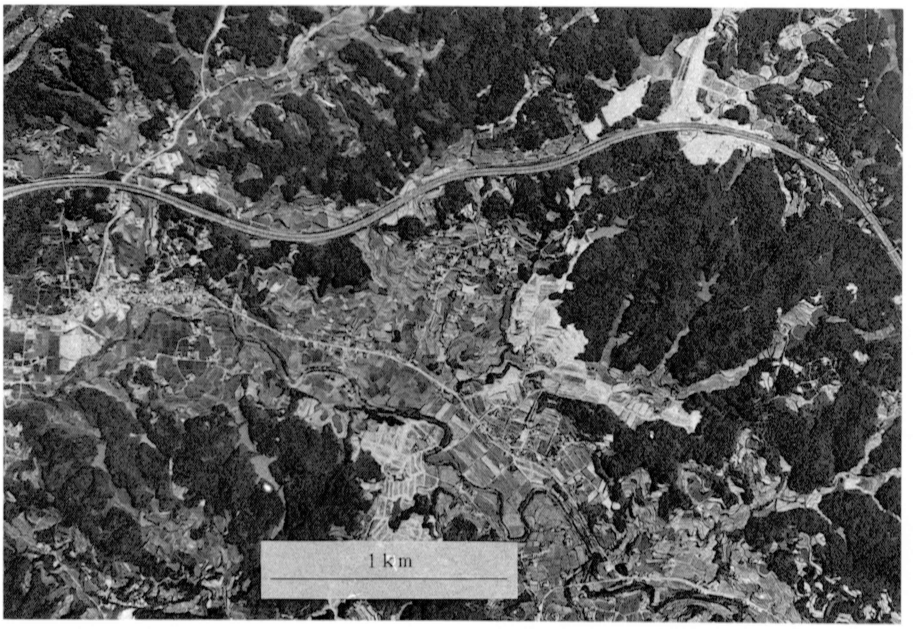

Plate 1. Aerial photograph of the Kinkai area.

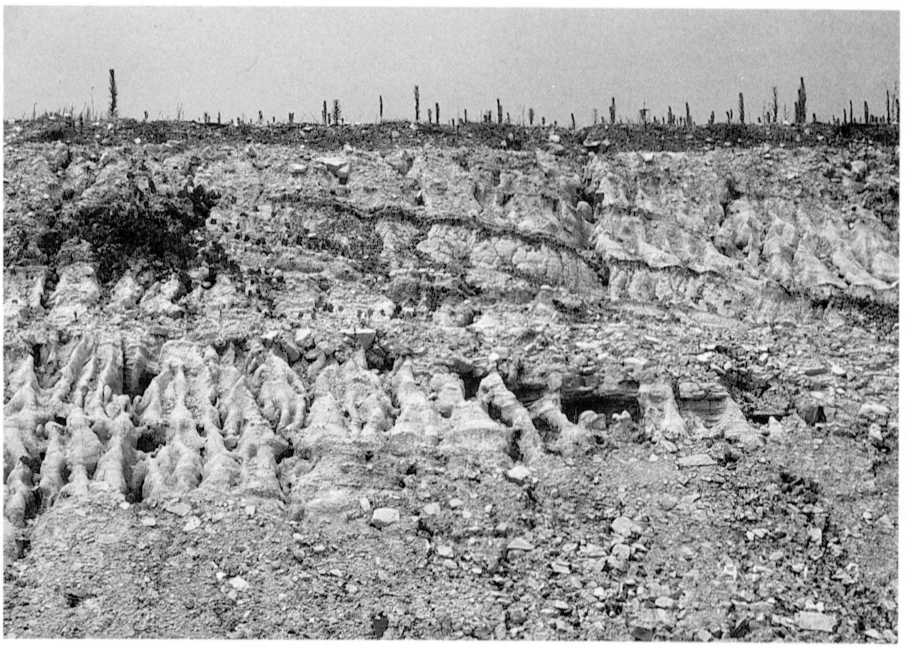

Plate 2. Outcrop of the Kinkai area.

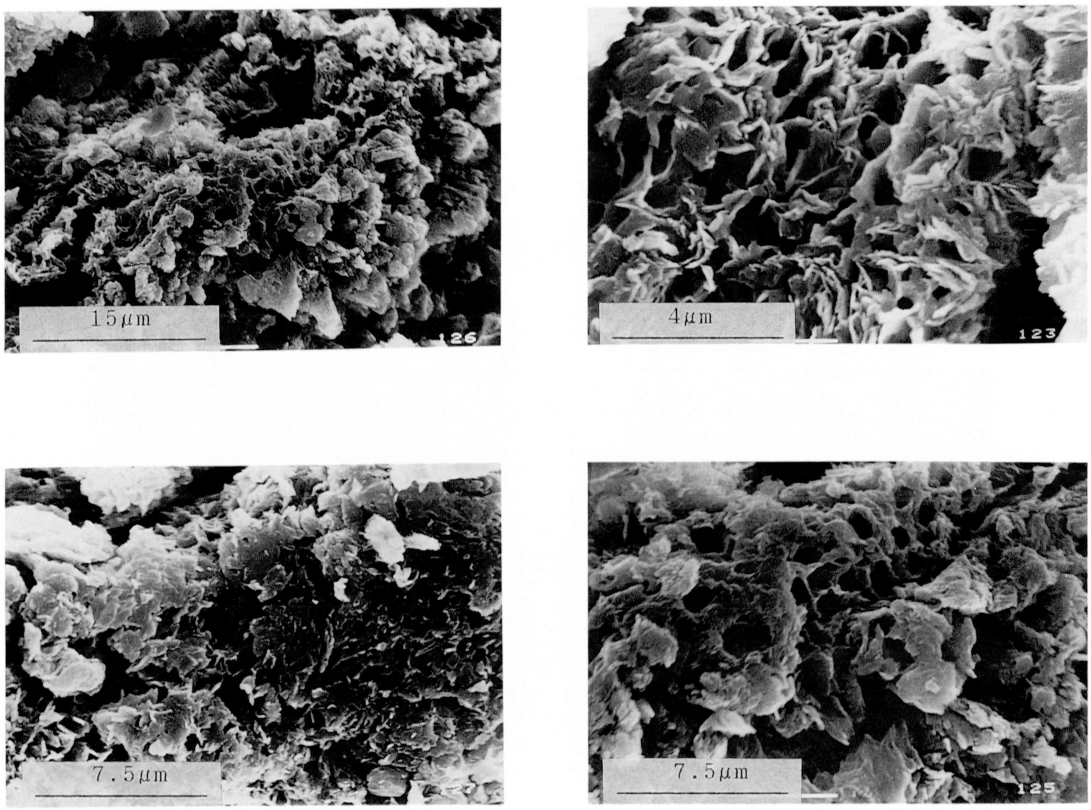

Plate 3. Scanning electron micrographs of montmorillonite in the Kinkai area.

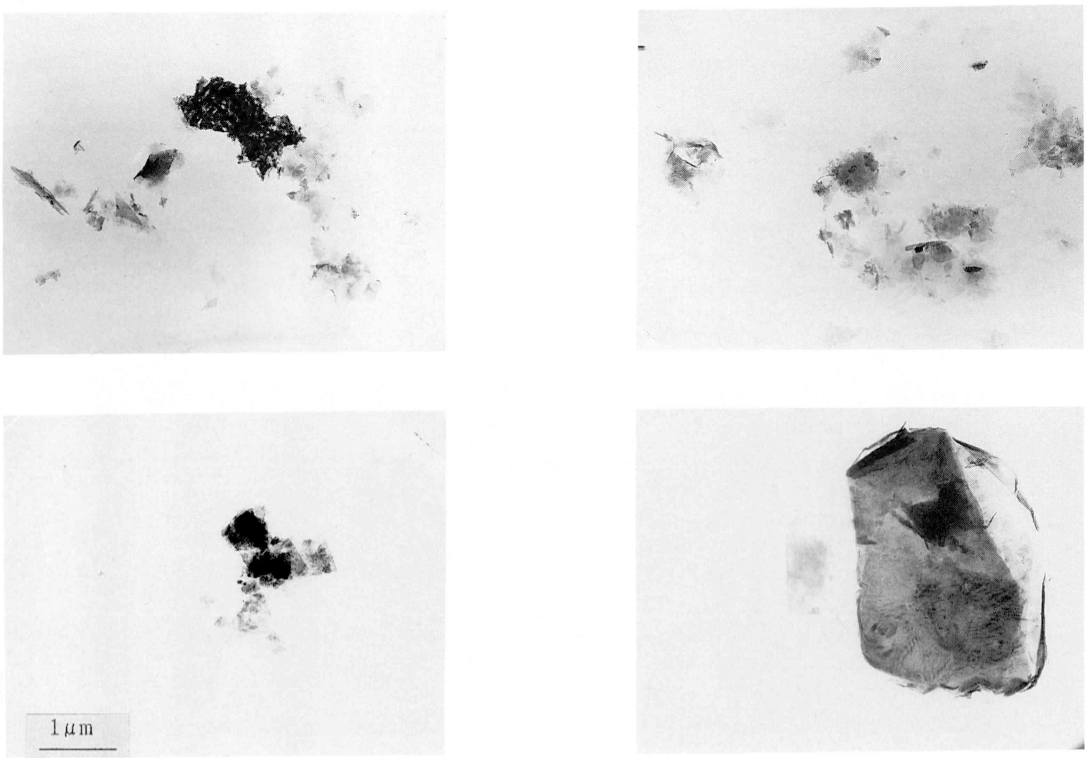

Plate 4. Transmission electron micrographs of montmorillonite in the Kinkai area.

Plate 5. Slickenside in the D bed.

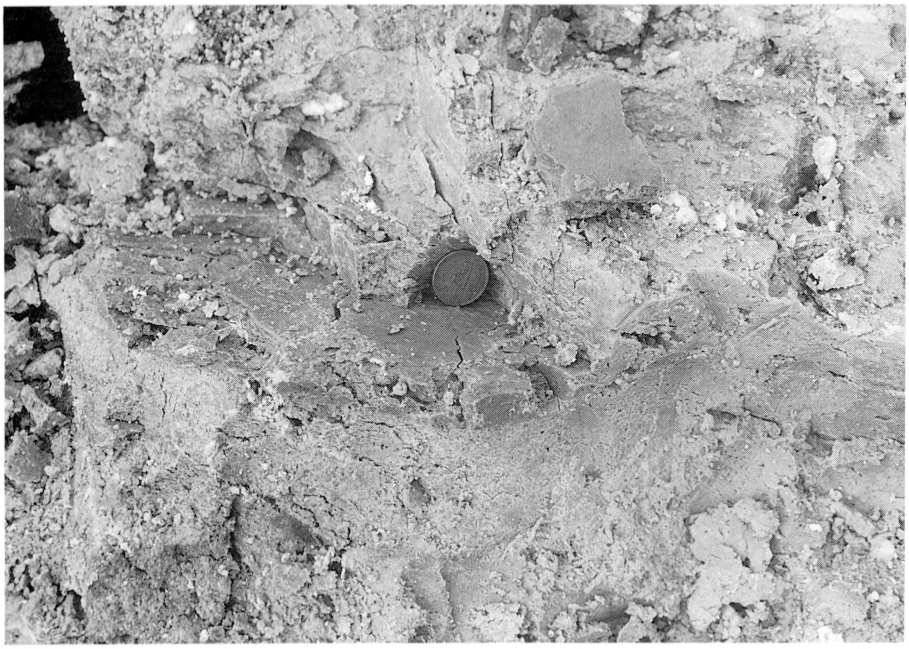

Plate 6. The D bed after rainfall.